

# BER Analysis of an 8 x 8 Open-loop MIMO system over Nakagami-m fading channel

Ritaban Biswas<sup>1</sup>, Niloy Ghosh<sup>2</sup>, Souvik Maji<sup>3</sup>

<sup>1</sup>(Department of Electronics and Communication Engineering, Haldia Institute of Technology, Haldia, India)

<sup>2</sup>(Department of Electronics and Communication Engineering, Haldia Institute of Technology, Haldia, India)

<sup>3</sup>(Department of Electronics and Communication Engineering, Haldia Institute of Technology, Haldia, India)

---

**Abstract:** The Bit Error Rate (BER) analysis of wireless communication systems over fading channels is an important performance metric for establishing the transmission quality (i.e., quality of service) across fading channels. Having a closed form formulation that can determine BER performance as a function of wireless channel stats and system parameters is a critical finding that many academics are striving to acquire (e.g., modulation order). These closedform expressions will make it a lot easier to design, execute, and test wireless systems. The objective of this paper is to perform BER Analysis of an 8 x 8 Open-loop MIMO system over Nakagami-m fading channel. This has been established through the implementation of Spatial Multiplexing and the use of Q-function & its various approximations. The overall approach is mathematical in nature. Lastly, the simulation results have been displayed by  $Q(x)$  v/s.  $\alpha$  curves, suggesting which approximation is the most effective one. All simulations, plots and analyses have been implemented using MATLAB®.

**Key Word:** Fading, Nakagami-m fading model, MIMO, BER analysis, Spatial Multiplexing, Wireless Communication

---

Date of Submission: 14-11-2022

Date of Acceptance: 28-11-2022

---

## I. Introduction

Due to the existence of numerous types of objects in the proximity, a signal travelling through wireless media undergoes a variety of physical processes. These outdoor items are primarily made up of mobile and immobile obstacles with varying physical qualities. Depending on the nature and size of the obstruction, as well as the frequency of the signal, various signal properties such as phase and amplitude are modified following impact with such impediments.

As a result of numerous processes such as reflection, diffraction, and scattering, the received signal is a collection of multiple components. This causes a brief fluctuation in the amplitude and power levels of the received signal. When the transmitter, receiver, and/or the surrounding objects are moving, these fluctuations in the received power level become more severe. Furthermore, the type of the surrounding objects has a considerable impact on the variability in the received power level. This variation is random, and it may be described using a variety of probability distributions that vary based on the situation. Fading is the term for a change in received power through time and space. In many circumstances, detailed analysis of such variances is extremely difficult, if not impossible.

The analysis can be simplified by statistical modelling of received power or amplitude using various distributions. Depending on the type of fading, the statistical modelling may differ. In the frequency domain, fading can be characterized as frequency flat fading or frequency selective fading. Both types of fading have different statistical modelling.

The different types of fading and how they relate to the rate of change of channel parameters will be briefly reviewed. Following that, there will be a review of some well-known statistical models for fading distributions and their relevance in various wireless contexts. After that, the generalized fading distributions will be considered. It includes information on the physical models that can be studied and represented, as well as statistical aspects that can be beneficial in wireless communication system analysis.

There will also be special examples of the generalized fading distributions. The methods for generating fading channel coefficients that follow generalized fading distributions are also covered in this chapter. When modelling wireless communication systems, these channel coefficients are useful.

The channel conditions have a big impact on the fading characteristics. The coherence bandwidth and coherence time of the channel are the two characteristics used to classify fading channels. The Doppler shift and delay spread of the multipath components, respectively, determine coherence time and bandwidth. Doppler shift happens when the transmitter and receiver are moving relative to each other while communicating. The

transmitter and receiver may be moving closer or farther apart as they move. As a result, the Doppler shift could be either positive or negative. This effectively boosts or decreases the signal's frequency.

The relation between Doppler spread and coherence time can be given as the following-

$$T_c = 1/f_d$$

where  $f_d$  is the maximum Doppler spread, and  $T_c$  is the channel's coherence time. Coherence time is defined as the amount of time during which the channel's impulse response does not vary. Another feature of fading channels is their coherence bandwidth. It is the frequency response of a channel that is constant or flat over a certain range of frequencies. The maximum delay spread of multipath components is proportional to the channel's coherence bandwidth.

As an example, consider the following relationship:

$$f_c = 1/\tau_d$$

where  $f_c$  is the coherence bandwidth and  $\tau_d$  is the maximum delay spread.

The fading phenomena can be divided into two categories: large-scale fading and small-scale fading. When a mobile phone moves over a large distance, such as a distance on the order of a cell size, large-scale fading happens. It's produced by signal channel loss as a function of distance, as well as shadowing from large objects like buildings, intervening terrains, and vegetation. Shadowing is a slow fading phenomenon in which the median path loss between the transmitter and receiver in fixed sites varies. In other words, average path loss and shadowing describe large-scale fading. Small-scale fading, on the other hand, is the fast change in signal levels caused by the constructive and destructive interference of numerous signal routes (multi-paths) while the mobile station moves short distances. For small-scaling fading, the frequency selectivity of a channel is characterized (e.g., by frequency-selective or frequency-flat) depending on the relative degree of multipath. Meanwhile, short-term fading can be classed as fast or slow fading depending on the time variation in a channel caused by mobile speed (as measured by the Doppler spread).

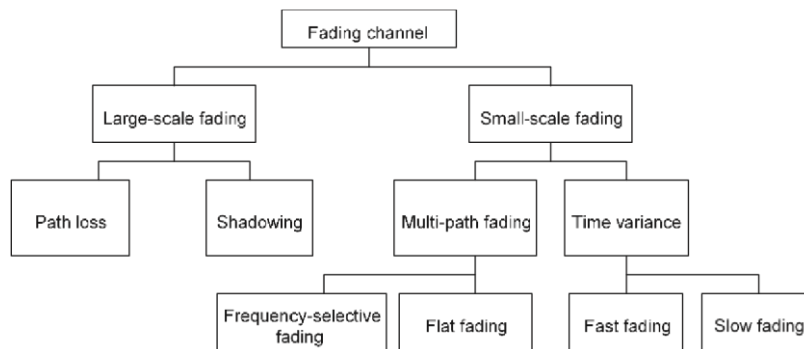


Fig. 1.1: Classification of fading channels.

## II. Nakagami-m Fading

In various settings, the Nakagami-m distribution is used to model fading scenarios (mostly in a non-LOS environment). Because of the ease of analysis, it is often investigated by researchers. The Nakagami-m distribution is also often used to represent received signal fading statistics, however it can only model fading under generalised conditions to a certain extent. As a result, we classed Nakagami-m fading as a generalised fading model in this section.

**2.1 Physical Model:** We will explore the physical reality of the Nakagami-m distribution in this section of the debate. Understanding the real physical modelling of wireless channels, as well as the application of the Nakagami-m distribution in statistical modelling of fading channels, is critical. The received signal is treated as a collection of clusters in the Nakagami-m fading model. A number of distributed multipath components make up each cluster. The delay spread of multipath components within a cluster is bigger than the delay spread of separate clusters. The power of each cluster is expected to be the same. The fading signal's envelope  $X$  can be represented as in this model, by:

$$X^2 = \sum_{i=0}^n (I_i^2 + Q_i^2)$$

where,  $n$  is the number of clusters in the received signal, and  $I_i$  and  $Q_i$  are respectively the in-phase and quadrature phase component of the resultant signal of the  $i^{th}$  cluster.  $I_i$  and  $Q_i$  are mutually independent random processes with zero mean and equal variance. Both  $I_i$  and  $Q_i$ , being resultant of multipath components of a cluster, may be assumed to be Gaussian distributed with  $E(I_i) = E(Q_i) = 0$  and  $E(I_i^2) = E(Q_i^2) = \sigma^2$ .

From the fact that  $I_i$  and  $Q_i$  are Gaussian distributed, it is to be noted here that each  $R_i^2$  is exponentially distributed. The SNR in this case is the sum of mutually independent Gamma distributed random variables. The PDF of SNR follows Gamma distribution and can be given as:

$$P_\gamma(\gamma) = \frac{m^m \gamma^{(m-1)}}{\bar{\gamma}^m \Gamma(m)} e^{-\frac{m\gamma}{\bar{\gamma}}}, \quad \gamma \geq 0$$

where  $\Gamma(\cdot)$  is the Gamma function and  $m$  is the fading parameter given by:

$$m = \frac{(E(X^2))^2}{E(X^2) - E(X)^2}, \quad m \geq 0.5$$

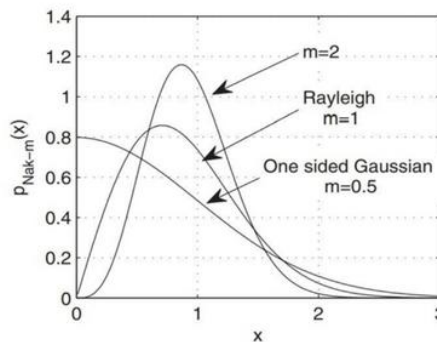


Fig. 2.1: PDFs of some special cases of Nakagami-m distribution.

### III. Bit-Error Rate (BER) of MIMO systems, incorporating fading channels

The bit-error rate, or BER, is a key metric for assessing the performance of data channels. The crucial parameter for transmitting data from one point to another, whether via radio/wireless or cable telecommunications, is how many errors will occur in the data at the remote end. As a result, BER is relevant to a wide range of technologies, including fiber optic lines, ADSL, Wi-Fi, cellular communications, IoT networks, and many more. Even if the data channels use many different types of technology, the fundamentals of calculating the bit error rate are the same.

There is a chance that errors will be introduced into the system when data is transmitted across a data link. If errors are introduced into the data, the system's integrity may be jeopardized. As a result, it's important to evaluate the system's performance, and the bit error rate, or BER, is an excellent way to do so. BER evaluates the whole end-to-end performance of a system, including the transmitter, receiver, and the medium between them, unlike many other types of evaluation. In this approach, the bit error rate, or BER, can be used to test the real performance of a system in use, rather than just the component pieces and hoping they work properly.

A bit error rate is the rate at which errors occur in a transmission system, as the name implies. This can be easily translated into the number of errors in a string of a specified length. If the medium between the transmitter and receiver is good and the signal to noise ratio is strong, the bit error rate will be very low - perhaps inconsequential and have no influence on the entire system. However, if noise is discovered, the bit error rate may need to be considered. Noise and variations in the propagation path are the main causes of data channel deterioration and BER (where radio signal paths are used). Both effects are random, with the noise using a Gaussian probability function and the propagation model using a Rayleigh model. This means that statistical analytic techniques are typically used to analyze channel properties.

**3.1 BER and  $E_b/N_0$ :** Radio connectivity and radio communications systems are more closely related with signal to noise ratios and  $E_b/N_0$  statistics. The bit error rate, or BER, can alternatively be expressed in terms of probability of error, or POE. Three more criteria are utilized to determine this. They are the error function, *erf*, the energy in a single bit,  $E_b$ , and the noise power spectral density,  $N_0$ . It should be noted that the error function has a different value for each form of modulation. Because each sort of modulation behaves differently in the presence of noise, this is the case. Larger order modulation techniques (for example, 64-QAM) that may transport higher data rates are less resistant in the presence of noise. Lower-order modulation schemes (such as BPSK, QPSK, and others) have lower data speeds but are more reliable. The energy per bit,  $E_b$ , is a measure of energy in Joules that may be calculated by dividing the carrier power by the bit rate.  $N_0$  is a power per Hertz; hence this has power (joules per second) divided by seconds as dimensions. When the dimensions of the ratio  $E_b/N_0$  are added together, they provide a dimensionless ratio. It's vital to remember that POE is a signal-to-noise ratio that is proportional to  $E_b/N_0$ .

The bit error rate can be expressed in terms of a likelihood of error:

$$POE = \frac{1}{2}(1 - erf) \sqrt{\frac{E_b}{N_0}}$$

where, *erf* is the error function,  $E_b$  is the energy in one bit and  $N_0$  is the power spectral density (noise in 1 Hz bandwidth).

**3.2 Spatial Multiplexing:** The incoming data stream is transformed from serial to parallel for transmission in spatial multiplexing. The parallel streams of data obtained following this conversion are broadcast simultaneously from the transmitter's many antennas. This has two major implications for wireless communication systems in practise.

- If data is transferred simultaneously at the same pace as it is generated, bandwidth requirements are reduced. This is more useful for data transmission in real time.
- The number of transmitting antennas influences the effective data rate. This speeds up total communication. This is useful when sending data that has already been saved (more towards the applications of internet or for multimedia transmission).

In comparison to systems with a single transmitter antenna, the transmission rate is multiplied by the number of antennas available at the transmitter.

Until the emergence of MIMO systems, multipath/scattering and fading were considered shortcomings. The benefits of a rich scattering environment for MIMO systems are demonstrated in the following example. Consider a two-way MIMO network. It transmits data using the BPSK modulation technique. Assume that multipath fading does not exist. All channel coefficients are unity in the absence of fading. Thus, the channel matrix is of size  $2 \times 2$  with all entries equal to '1', i.e.,  $H = [1 \ 1 \ | \ 1 \ 1]$ . Let, the groups of two incoming bits at a time be '0, 0', '0, 1', '1, 0' or '1, 1'. Using BPSK they will be respectively mapped as  $x_1 = [-1 \ | \ -1]$ ,  $x_2 = [-1 \ | \ 1]$ ,  $x_3 = [1 \ | \ -1]$ ,  $x_4 = [1 \ | \ 1]$ , which can also be called transmitted codewords.

Both the BPSK-modulated bits will be transmitted simultaneously from the two antennas at the transmitter. Received signal at both the receive antennas in absence of noise for each of the cases may be given by  $r_i = H \cdot x_i$ , which can respectively be represented as  $r_1 = [-2 \ | \ -2]$ ,  $r_2 = [0 \ | \ 0]$ ,  $r_3 = [0 \ | \ 0]$  and  $r_4 = [2 \ | \ 2]$ .

The receiver can only successfully decode the symbols when the broadcast bits/symbols from each of the transmitter antennas are the identical, as shown in the previous example. The received vectors in the other two circumstances are identical in both cases. Even in the absence of noise, a correct decision is impossible. However, in all circumstances, there is the chance of inaccuracy in noisy conditions.

The detected symbol is obtained as follows for detection at the receiver using the maximum likelihood (ML) rule, which provides the best performance in terms of BER/symbol error rate (SER).

$$i_d = \underset{j}{\operatorname{arg\,min}} |\mathbf{r} - \mathbf{H}\mathbf{x}_j|^2$$

where,  $i_d$  is the index of the detected vector when received vector is  $r$ . So, the detected vector at the receiver becomes  $x_{i_d}$ .

Thus, spatial multiplexing can be summed up in the following three points:

- All the antennas at transmitter are used to transmit the data streams in parallel.
- Transmission rate enhances linearly with number of transmitter antennas.
- The diversity order depends only on the number of antennas at the receiver and independent of antennas at the transmitter.

#### IV. Experimental Procedure

In the previous sections, we discussed about the relevant fading models, the MIMO Systems that work with channel models, an introductory discussion of BER & SNR, and Spatial Multiplexing, a paradigm of Open-loop MIMO systems. In this section, a simple and accurate generalized closed-form equation for the bit error rate (BER) over the Nakagami-m fading channel (for an 8 x 8 Spatially Multiplexed MIMO system) is developed based on Chiani, Dardari, and Simon's approximated expression of the Q-function. The formula is a product of the well-known gamma function and the Nakagami-m fading parameter's finite sum of functions. The obtained expression is valid for any real 0.5 and any order of coherent modulation method. Using various combinations of modulation orders and Nakagami-m fading settings, numerical results are used to validate the resulting formulas.

**4.1 Mathematical Derivations:** By averaging the BER of the AWGN channel with the PDF of the fading envelope, the BER due to fading channel can be determined. As a result, the Q-function is frequently used in the resultant expression of this averaging procedure. In the AWGN channel, consider the expression of the SER of various modulation schemes to be:

$$SER = \varphi Q(\sqrt{\kappa\gamma})$$

where,  $Q(\cdot)$  is the Q-function defined by:

$$Q(x) = \int_x^\infty \frac{1}{\sqrt{2\pi}} \exp\left(-\frac{u^2}{2}\right) du$$

and  $\varphi$  and  $\kappa$  are constants that depends on the modulation scheme.

**Table no. 1:** Values of  $\varphi$  and  $\kappa$  for different schemes.

Modulation Scheme	SER	$\varphi$	$\kappa$
BFSK	$= Q(\sqrt{\gamma})$	1	1
BPSK	$= Q(\sqrt{2\gamma})$	1	2
QPSK,4-QAM	$\approx 2Q(\sqrt{\gamma})$	2	1
M-PAM	$\approx \frac{2(M-1)}{M} Q\left(\sqrt{\frac{6}{M^2-1}\gamma}\right)$	$\frac{2(M-1)}{M}$	$\frac{6}{M^2-1}$
M-PSK	$\approx 2Q\left(\sqrt{2\sin^2\left(\frac{\pi}{M}\right)\gamma}\right)$	2	$2\sin^2\left(\frac{\pi}{M}\right)$
Rectangular M-QAM	$\approx \frac{4(\sqrt{M}-1)}{\sqrt{M}} Q\left(\sqrt{\frac{3}{M-1}\gamma}\right)$	$\frac{4(\sqrt{M}-1)}{\sqrt{M}}$	$\frac{3}{M-1}$
Non-Rectangular M-QAM	$\approx 4Q\left(\sqrt{\frac{3}{M-1}\gamma}\right)$	4	$\frac{3}{M-1}$

Hence, the SER (and hence the BER) can be obtained by averaging the *Q-function* and the PDF of the *Nakagami-m fading* model, which is:

$$P_e = \int_0^\infty \varphi Q(\sqrt{\kappa\gamma}) p_\gamma(\gamma) d\gamma$$

$$= \varphi \frac{m^m}{\gamma^m \Gamma(m)} \int_0^\infty Q(\sqrt{\kappa\gamma}) \gamma^{(m-1)} \exp\left(-\frac{m\gamma}{\bar{\gamma}}\right) d\gamma$$

The main aim now is evaluating the integration given above and find closed-form expression. The aforesaid integration involves the *Q-function* which is difficult to integrate. Thus, in literature, there are many approximations of the *Q-function* with different degrees of accuracy and complexity.

In the equation given below, four types of approximations of the *Q-function* are given, based on parameters and circumstances.

- **GKAL Approximation:** The accuracy of the expression can be adjusted by modifying A and B, but the optimum values of A and B are A = 1.98 and B = 1.135, respectively, and we will refer to this approximation by GKAL.

$$Q(x) \approx \frac{(1 - e^{\frac{Ax}{\sqrt{2}}}) e^{-\frac{x^2}{2}}}{\sqrt{2\pi Bx}}$$

- **PBCS Approximation:** This approximation does not consider any parameter hence this is less popular in use and implementation.

$$Q(x) \approx \frac{e^{-\frac{x^2}{2}}}{\sqrt{2\pi} \sqrt{1+x^2}}$$

- **OPBCS Approximation:** The accuracy of the expression can be adjusted by modifying A and B, but the optimum values of a and b are a = 0.339 and b = 5.510, respectively,

$$Q(x) \approx \frac{1}{(1-a)x + a\sqrt{b+x^2}} \cdot \frac{e^{-\frac{x^2}{2}}}{\sqrt{2\pi}}$$

- **CDS Approximation:** The accuracy can be further improved by adding more exponentials to a modified OPBCS Approximation.

$$Q(x) \approx \frac{e^{-\frac{x^2}{2}}}{12} + \frac{e^{-\frac{2x^2}{3}}}{4}$$

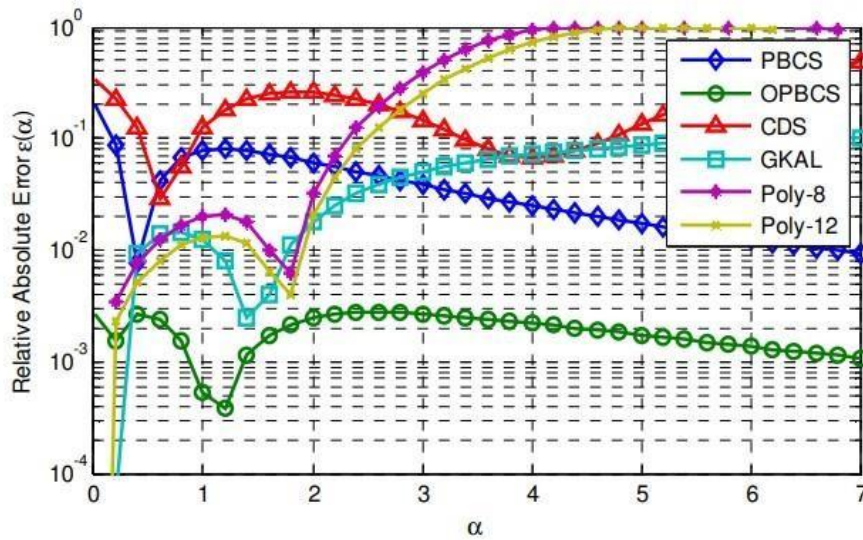


Fig. 4.1: Absolute relative error for different approximations of the Q-function, PBCS, OPBCS, CDS, GKAL, and the Polynomial approximation for n=8 and n=12.

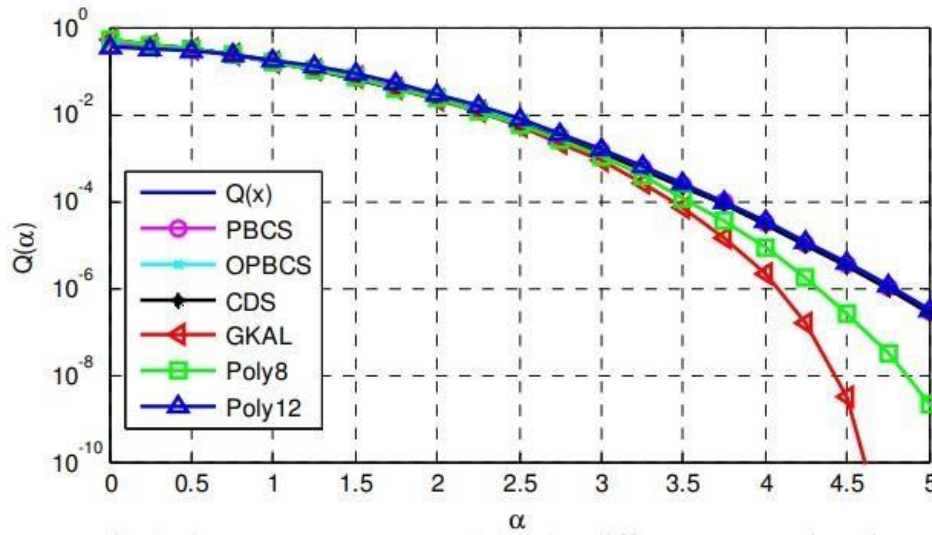
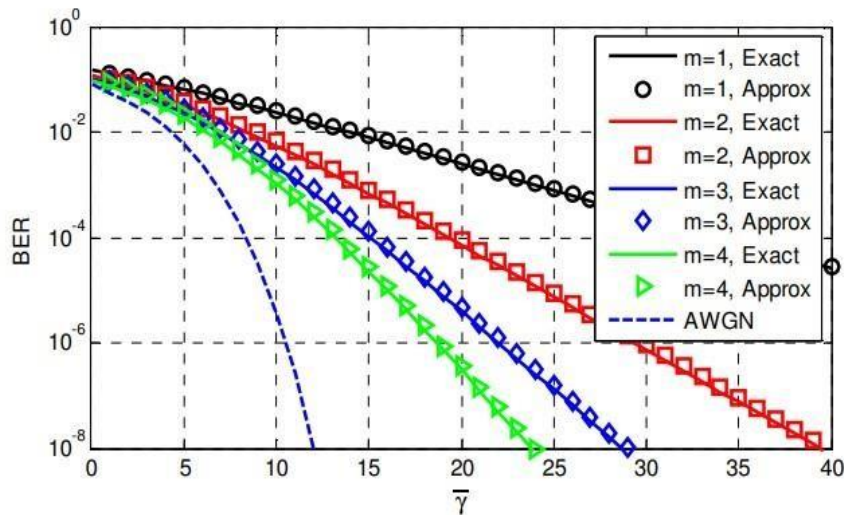


Fig. 4.2: Q(x) curves generated by the different approximations.

### V. Simulation Results

The probability of the error expression derived above can be used now to evaluate the performance in terms of BER over *Rayleigh fading* channel ( $m=1$ ) as well as *Nakagami-m fading* channel for any modulation scheme by simply choosing the appropriate values of  $\varphi$  and  $\kappa$  from Table no. 1.

Testing the expression derived above is conducted using three different scenarios. First, we choose a modulation scheme from Table 3.1 (Binary Phase Shift Keying) and test the performance over different values of Nakagami-m fading parameters, specifically  $m=1, 2, 3$  and  $4$ . Numerical results for equation which represents the exact BER curve were compared with the approximated BER curve that has been evaluated using the expression in the previous section. The results are shown in Fig. 5.1. It can be seen that the approximated expression is highly accurate and matches the numerical results for different values of  $m$  as well as different values of  $\gamma$ .



**Fig. 5.1:** BPSK over Nakagami-m fading channel, evaluated for  $m=1$  (Rayleigh), 2, 3 & 4 and compared with numerical results.

The second testing scenario is mainly by using the expression for the same modulation scheme, (we've chosen Rectangular M-QAM), but with different modulation orders over a fixed value of  $m$  ( $m=1$ , i.e., Rayleigh Fading Channel). 4-QAM, 16-QAM and 64-QAM were used and the results are shown in Fig. 5.2. The accuracy of the derived expression in Section 3.2 compared to the numerical results formerly is found to be very high.

As final investigation, the POE expression will be verified by observing its performance in a scenario where the BER curves of 4-QAM (i.e., QPSK) and 32-QAM will be evaluated by numerically integrating (7) and comparing the curves with those generated in the previous section for two values of fading parameter  $m$ , specifically  $m=1$  and  $m=2.1$ . The results are shown in Fig. 5.3.

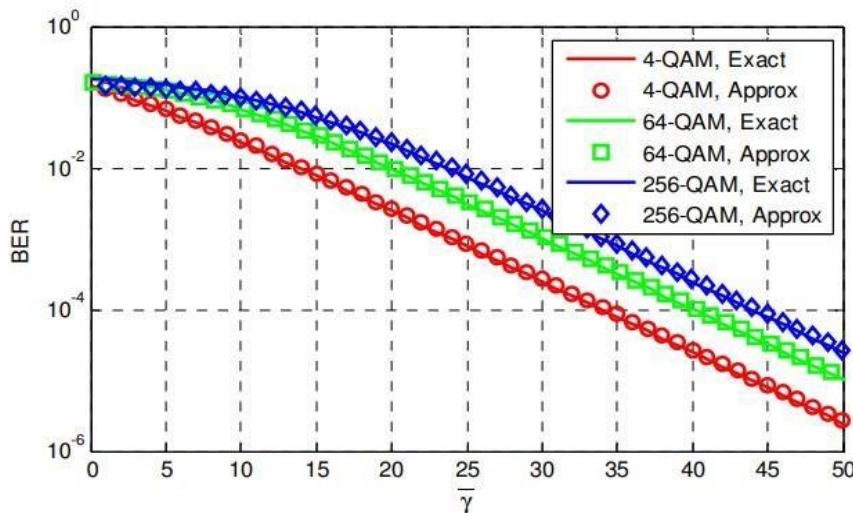


**Fig. 5.2:** 4-QAM, 16-QAM and 64-QAM over Nakagami-m Channel with  $m=1$  (Rayleigh).

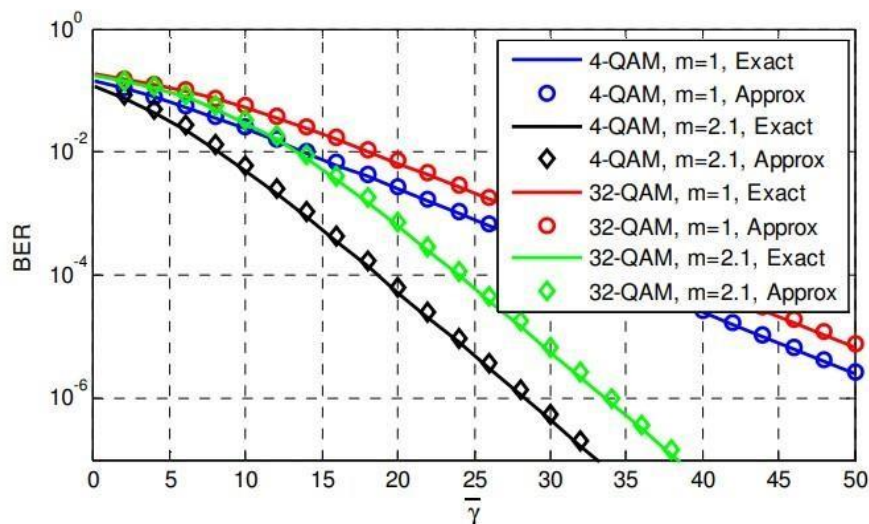


**Fig. 5.3:** Comparison between 4-QAM (QPSK) and 32-QAM bit BER performance over *Nakagami-m* channel,  $m=0.9, 0.5$  and  $2.1$ .

## V. Discussion

Over *Nakagami-m* fading channels, a simple and extremely accurate generalised closed-form equation for the BER is found using the *CDS approximation* of the *Q*-function. The obtained expression was verified using numerical findings for a variety of circumstances in which the BER curves closely matched the exact values. The developed expression's correctness and simplicity make it a good option for researchers in various fields to utilise in evaluating the performance of MIMO systems over *Nakagami-m* fading channels.

## VII. Conclusion

Generalized fading channels are rather recent channel models. The beauty of the generalized fading distributions is that all the previous fading distributions like Rayleigh, Rician, Weibull, etc. are cases of them. MIMO wireless communications is one of the biggest advancements in the wireless communications. MIMO systems can achieve rate and diversity gains over SISO systems without penalty in bandwidth and signal power. There has been a sizable number of research papers in MIMO wireless communications over generalized fading channels.

Fading models, that are incorporated in MIMO systems, are altogether the technique underpinning the RADAR communications system, in addition to the smart antenna systems used in fixed and cellular transmission. By estimating the reflection of radio signals transmitted to it, the passive radar uses an advanced signal processing technique to determine the distance between itself and a distant object. In the Second World War, passive radar was commonly used to identify Nazi aircraft approaching the United Kingdom. A transmitter sends radio signals in the form of waves in numerous directions in traditional radar. The signal will be reflected back to the receiving antenna if any target (aircraft) is within the transmission's radius. The radar's mechanism is a variation of the MIMO technology.

MIMO is already employed in fourth generation (4G) mobile and it will be fully utilized in fifth generation (5G) mobile. This is why we have implemented MIMO systems throughout this thesis project. The three big pillars of 5G, viz. massive MIMO, millimeter wave (mmWave) and small cell networks, are for further scrutinization. As an advanced paradigm, device-to-device (D2D) communications for internet of things (IoT) will take an immense aid from MIMO systems using fading models.

MIMO technology is a key component of next-generation wireless technologies because it provides higher gains and throughputs than other approaches. Aside from high throughputs, its capacity to overcome wireless technology's flaw (multipath interference) has positioned it as the future of modern wireless transmission technology.

### References

- [1]. V. Aggarwal, Jagadish Chandra Bose: The real inventor of Marconis wireless receiver. *The Ancient Wireless Association Journal*, 47(3):50–54, July 2006.
- [2]. S. M. Alamouti. A simple transmit diversity technique for wireless communications. *IEEE Journal on Selected Areas in Communications*, 16(8):1451–1458, Oct 1998.
- [3]. M. S. Alouini and A. J. Goldsmith. Capacity of Rayleigh fading channels under different adaptive transmission and diversity-combining techniques. *IEEE Transactions Vehicular Technology*, 48(4):1165–1181, July 1999.
- [4]. J. G. Andrews, S. Buzzi, W. Choi, S. Hanly, A. Lozano, A. C. K. Soong, and J. Zhang. What will 5G be? *IEEE Journal on Selected Areas in Communications*, 32(6):1065–1082, 2014.
- [5]. O. S. Badarneh and R. Mesleh. Spatial modulation performance analysis over generalized  $\eta - \mu$  fading channels. In *24<sup>th</sup> IEEE International Symposium on Personal Indoor and Mobile Radio Communications (PIMRC)*, pages 886–890, Sept 2013.
- [6]. L. Bai and J. Choi. *Low Complexity MIMO Detection*. Springer Science & Business Media, 2012.
- [7]. E. Basar, U. Aygolu, E. Panayirci, and H. V. Poor. Space-time block coded spatial modulation. *IEEE Transactions on Communications*, 59(3):823–832, March 2011.
- [8]. A. Bhowal and R. S. Kshetrimayum. End to end performance analysis of m2m cooperative system over cascaded  $\alpha - \mu$  channels. In *Proceedings of the International Conference on COMMunication Systems & NETWORKS*, pages 1–7. IEEE, 2017.
- [9]. E. Bjornson, E. G. Larsson, and T. L. Marzetta. Massive MIMO: Ten myths and one critical question. *IEEE Communications Magazine*, 54(2):114–123, 2016. P. K. Bondyopadhyay. Under the glare of a thousand suns — the pioneering works of Sir J. C. Bose. *Proceedings of the IEEE*, 86(1):218–224, Jan 1998.
- [10]. R. Brandt. *Coordinated Precoding for Multicell MIMO Networks*. KTH, Sweden, 2014.
- [11]. M. Chaudhury, N. K. Meena, and R. S. Kshetrimayum. Local search based near optimal low complexity detection for large MIMO system. In *Proceedings of the IEEE International Conference on Advanced Networks and Telecommunications Systems*, pages 1–5. IEEE, 2016.
- [12]. Y. Chen and C. Tellambura. Distribution functions of selection combiner output in equally correlated Rayleigh, Rician, and Nakagami- $m$  fading channels. *IEEE Transactions on Communications*, 52(11):1948–1956, 2004.
- [13]. Z. Chen, Z. Chi, Y. Li, and B. Vucetic. Error performance of maximalratio combining with transmit antenna selection in flat Nakagami- $m$  fading channels. *IEEE Transactions on Wireless Communications*, 8(1):424–431, Jan 2009.
- [14]. J. Choi. *Optimal Combining and Detection*. Cambridge University Press, Cambridge, 2010.

Ritaban Biswas. “BER Analysis of an  $8 \times 8$  Open-loop MIMO system over Nakagami- $m$  fading channel .” *IOSR Journal of Electrical and Electronics Engineering (IOSR-JEEE)*, 17(6), 2022, pp. 32-41.